RSC Advances

ROYAL SOCIETY OF CHEMISTRY

www.rsc.org/advances

Journal Name

ARTICLE

cRGD-Functionalized redox-sensitive micelles as potential doxorubicin delivery carriers for $\alpha_v\beta_3$ integrin over expressing tumors

Received 00th January 20xx,
Accepted 00th January 20xx

DOI: 10.1039/x0xx00000x

www.rsc.org/

Meng Cai [a], Mengyuan Ye [a], Xingxing Shang [a], Honghao Sun [a], Mingxing Liu [a], Hongmei Sun [a], Zhuo Ma [a,b] and Hongda Zhu [a,b]

Polymeric micelles as a nanocarrier-based drug delivery systems provide an innovative platform for selectively delivering active molecules and offer better antitumour activity. However, circulation stability in vivo, controllable drug intracellular release and high targeting efficiency are several practical challenges for micelles. Therefore, we developed cRGD-modified and shell crosslinked micelles (RSCMs) based on amphiphilic ploy (styrene-co-maleic anhydride) (SMA). RSCMs exhibited a spherical shape and homogeneous with an average diameter of 106.1 nm and a low polydispersity of 0.087. By comparisons, after crosslinking micelles possessed better stability to against dilution and stronger redox-response towards dithiothreitol (DTT). The SMA micelles displayed high drug loading capacity for hydrophobic DOX with a drug loading of approximately 14.1-19.2% (w/w) and an encapsulation efficiency of 72.1-82.7% (w/w). The *in vitro* release studies of shell crosslinked micelles showed that DOX release was minimal (＜25%, 24 h） under physiological conditions. However, in the presence of 10 mM DTT, accelerated release of DOX was achieved (60%, 24 h). MTT assays in B16F10 cells indicated that RSCMs displayed low cytotoxicity up to a concentration of 500 μg ml^{-1}. Moreover, the IC_{50} value showed that cRGD-DOX-ss-M could be more effective than other groups. *In vitro*, cellular uptake was further researched with confocal laser scanning microscopy and flow cytometry, both the qualitative and quantitative results demonstrated that cRGD-DOX-ss-M possessed much better specificity to cancer cells and superior stimulated release property in cytoplasm. Notably, cRGD-DOX-ss-M could more efficiently deliver and release into to the nuclei of $\alpha_v\beta_3$ integrin-overexpressing tumor cell line (B16F10) than counterparts of integrin-deficient tumor cells(Hela). Thus, these cRGD-modified redox-sensitive micelles have appeared as a high hopeful technology platform for targeted integrin-overexpressing tumor cells anticancer drug delivery and release.

1. Introduction

Chemotherapy is still the main treatment strategy for broad range of solid tumors.[1] However, clinical efficacy of therapies and survival benefit of the patient are limited by disadvantages of chemotherapeutic drugs such as low bioavailability, dose-limiting toxicities or drug delivery barriers.[2] Nanocarrier-based drug delivery systems (DDS) provide an innovative platform for selectively delivering active molecules and offer better antitumor activity,[3] among which polymeric micelles have emerged as a promising system, have been widely studied in preclinical[4, 5] and clinical trials.[6] Clinical studies have demonstrated that polymeric micelles overcame some limitations and delivered various drugs such as paclitaxel, doxorubicin or cisplatin[6-8] with remarkable antitumor efficacy. However, stability *in vivo*,[9, 10] controllable drug-release profiles[11]and high targeting efficiency of the tumor site[12-14] present several practical challenges for micelles as drug delivery systems.

To improve circulation stability of polymeric micelles and prevent drug leakage in blood circulation, the micelles could be crosslinked through a reversible bond under tumor microenvironment stimuli,[15] such as pH,[16,

[a] *School of Food and pharmaceutical Engineering, Key Laboratory of Fermentation Engineering (Ministry of Education), Hubei Provincial Cooperative Innovation Center of Industrial Fermentation, Hubei University of Technology, Wuhan 430068.*
[b] *Correspondence author: Hongda Zhu (Telephone: +86-27-59750481; E-mail: bszzhuhongda@yeah.net); Zhuo Ma (Email:mazhuo001789@sina.com).*

[17] redox signals[18-21] and multiple stimuli,[18, 22] which remain circulation stability and control activated drugs release in response to specific stimuli. Among the stimuli, redox potential is often used to trigger the intracellular drug delivery. Especially, disulfide crosslinking provides an opportunity for triggered drug to release due to the existence of abundant reducing substances including glutathione (GSH) in cancer cell,[23] which has recently been explored for reversible stabilization of polymeric micelles.[24] On the other hand, strategy to achieve cancer-targeted drug delivery is the utilization of unique cell-surface molecules markers that are specifically overexpressed in the cancerous tissues.[25] One such molecule such as the αvβ3 integrin, which can specifically recognize the peptide containing RGD (Arg–Gly–Asp) sequence, is a promising strategy for tumor-targeting treatment.[26] RGD receptors are overexpressed by tumor vessels and by a wide variety of human carcinoma cells including melanoma, breast, prostate, pancreas and colon. For example, RGD peptide analogues functionalized therapeutic systems such as micelles,[27, 28] liposome[29] and nanoparticle carriers[30, 31] have improved therapeutic efficiency and tumor selectivity.

In order to fully exert targeted antitumor effect and controllable drug-release of the drug delivery, we build RGD peptide analogues functionalized redox crosslinking polymeric micelles. Herein, we selected a cyclic pentapeptide c(Arg-Gly-Asp-d-Phe-Lys) (cRGDfK or named cRGD), which can selectively bind to αvβ3 integrin with high affinity,[27, 28] liganding to the surface of the micelles polymer. Hydrophobic doxorubicin (DOX) as a model drug was encapsulated into poly (styrene-co-maleic anhydride) micelles which were further crosslinked by cystamine to improve circulation stability and achieve redox-sensitive intracellular delivery (Fig. 1). Although the coupling of RGD peptides modified nanocarries were found to be able to target tumor blood vessels,[26] several strategies including circulation stability, controllable drug intracellular release and high targeting efficiency used in one polymeric micelles delivery system has not been reported. In this work, we evaluated the physicochemical properties of the cRGD-functionalized polymer micelles, and investigated stability against dilution, drug-release profile in response to the reducing environment of tumor cells. The effects of the micelles on cellular uptake were investigated in murine malignant melanoma cell line (B16F10) ($\alpha_v\beta_3$ integrin-positive) and human cervix adenocarcinoma cell line (Hela) ($\alpha_v\beta_3$ integrin- negative). It was expected that the cRGD-modified and redox-sensitive shell crosslinked micelles could increase the stability of the micelles in circulation, control drug intracellular release and enhance the targeted delivery of DOX into $\alpha_v\beta_3$ integrin over expressing tumor cells.

2. Materials and methods

2.1 Materials

Poly (styrene-co-maleic anhydride) (SMA, molecular weight 11760 Da) with a molar styrene to maleic anhydride ratio of 5:1 in the backbone was purchased from Polyscope Polymers Co, Ltd, (Geleen. Netherlands). c (RGDfK) peptide was synthesized by Shanghai ABBiocheem Co, Ltd, (Shanghai, China). Pyrene and 1,4-dithiothreitol (DTT) were purchased from Shanghai Aladdin Chemistry Co, Ltd, (Shanghai, China). Doxorubicin hydrochloride (DOX-HCl) was obtained from Xianghe shunda fine chemical Co, Ltd, (Wuhan, China). 3-(4,5-dimethylthiazol-2-yl)-2,5-diphenyl tetrazolium bromide (MTT), 4',6-diamidino-2-phenylindole (DAPI) and penicillin streptomycin were purchased from Biosharp (Hefei, China). RPMI-1640 and DMEM medium was purchased from Hyclone (Utah, USA). Trypsin was purchased from Gibco-BRL Life Technologies (Carlsbad, CA). Fetal bovine serum was purchased from Sijiqing Biology Engineering Materials Co, Ltd, (Zhejiang, China). All other chemicals used were analytical grade and used without further treatment.

2.2 Cell cultures

The mouse malignant melanoma cell lines (B16F10) and human cervix adenocarcinoma cell lines (Hela) were purchased from American Type Culture Collection (ATCC). The cells were cultured in RPMI-1640 and

DMEM medium respectively containing 10% (v:v) fetal bovine serum (FBS) and 1% antibiotics (penicillin G, 100 unit/ml; streptomycin, 100 unit/ml) at 37 °C in a 5% CO_2 atmosphere. At intervals, cells were passaged using 0.25% Trypsin-EDTA solution before confluence.

2.3 Micellar preparations

2.3.1 Preparation of SMA micelles and redox-sensitive shell crosslinked micelles

The non-crosslinked micelles (NCMs) were prepared by the conventional dialysis method.[32] Briefly, SMA (40 mg) was dissolved in 2 ml *N,N'*-dimethylformamide (DMF) and the solution(20 mg ml^{-1}) was added dropwise to 20 mlultra-pure water under stirring conditions. After the mixture was stirred for 1 h at room temperature (r.t.), DMF was isolated by dialysis (MWCO 14000) against 1 L deionized water for 24 h. The dialysis medium was refreshed at least 3 times. The shell crosslinked micelles (SCMs) were fabricated by the crosslinking of cystamine dihydrochloride. The molar ratio of maleic anhydride, cystamine dihydrochloride and sodium bicarbonate was 1:0.25:1. Firstly, 20 ml NCMs were catalytic hydrolysed by sodium bicarbonate (2.52 mg, 0.03 mM). After the suspension was stirred for 30 min, cystamine dihydrochloride (1.69 mg, 0.0075 mM) was added and further reacted for 12 h. Finally, the micelles were dialyzed against deionized water for 24 h to remove redundant crosslinker.

2.3.2 Preparation of cRGD-modified crosslinked micelles

The cRGD-modified crosslinked micelles (RSCMs) were prepared by one-step self-assembly method. Briefly, the NCMs was crosslinked by cystamine dihydrochloride as previously described. The molar ratio of maleic anhydride and cRGD peptide was 8:1, cRGD peptide (2.32 mg, 0.004 mM, 0.125 equiv. versus maleic anhydride) was added to the crosslinked micelles and incubated at 4 □ for 12 h. After incubation, the cRGD-modified crosslinked micelles were purified by dialysis.

2.3.3 Preparation of DOX-loaded micelles

DOX was chosen as a model drug to assess the DOX loaded NCMs (DOX-M), SCMs (DOX-ss-M) and RSCMs (cRGD-DOX-ss-M). The DOX-loaded polymeric micelles were prepared by dialysis method, while the whole procedure was performed in the dark. Typically, 2 ml of DOX-HCl solution in DMF (5.0 mg ml^{-1}) was pretreated by 20 µl of triethylamine for 6 hours. Then SMA (20 mg ml^{-1}) and DOX (5 mg ml^{-1}) dissolved in DMF were added dropwise to 20 ml ultra-pure water, stirring for 5 h at r.t. to allow for drug encapsulation. In the end, the mixture was dialyzed to eliminate unload DOX and the organic solvent. Then DOX-loaded micelles were crosslinked and modified as described in 2.3.1 and 2.3.2.

2.4 Characteristics of micelles

2.4.1 Determination of critical micellar concentration

The critical micellar concentration (CMC) of RSCMs was determined using pyrene as a fluorescent probe. The concentration of the block polymer was varied from 1×10^{-5} to 1 mg ml^{-1} and the concentration of pyrene was fixed at 0.6 µM. Fluorescence spectra were recorded using a fluorescence spectrometer (PerkinElmer LS55, USA) with an excitation wavelength of 334 nm. The emission fluorescence at 373 and 384 nm was monitored. The CMC was estimated at the crosspoint when extrapolating the intensity ratio I_{384}/I_{373} in low and high concentration regions.

2.4.2 Measurement of zeta potential, size distribution and TEM

The size and zeta potential of micelles were determined using dynamic light scattering (DLS). Measurements were carried out at 25 □ by a Zetasizer Nano-ZS90 (Malven, Worcestershire, UK) with a 632.8 nm He-Ne laser using back-scattering detection. The shape of micelles was observed using transmission electron microscopy (TEM, JEOL JEM-2100F, Japan) at an accelerating voltage of 200 kV. The samples were prepared by casting one drop of micelle suspension on

carbon-coated copper grids, followed by staining with 1 % phosphotungstic acid.

2.4.3 Stability of non-crosslinked micelles and shell crosslinked micelles

Physical stability of the NCMs and SCMs were investigated by DLS. The samples were diluted by organic solvent (DMF, 1:10) and extensive dilution (water, 1:5000), their size were measured by dynamic light scattering (DLS). The redox-responsiveness evaluation of SCMs in responsive to a reductive environment *in vitro* was monitored by DLS measurement. The sample solution at a concentration below the CMC was bubbled with N_2 for 15 min. Then, DTT was added to yield the final DTT concentration of 10 mM, the operation was in a shaking bed at 200 rpm and 37 ℃. The change of micelle size was determined by DLS at predetermined time intervals.

2.4.4 Detection of drug loading content and drug loading efficiency

To determine drug loading content (DLC) and drug loading efficiency (DLE), various DOX formulations were centrifuged at 10,000 rpm for 30 minutes to collect sediments and washed off the surface residual DOX. Then the sediments were freeze-dried to obtain the weights of DOX loaded micelles. The freeze-dried powders were dissolved in DMSO and determined by measuring the fluorescent intensity (excitation: 482nm, emission: 556nm) using a fluorescence spectrophotometer-(PerkinElmer LS55, USA). Wherein, calibration curve was obtained with DOX/DMSO solutions with different DOX concentrations. The DLC and DLE were calculated according to the following equations:

DLC (%) = (weight of loaded DOX / weight of DOX loaded micelles) × 100%

DLE (%) = (weight of loaded DOX / weight of added DOX) × 100%

2.5 *In vitro* drug-release behaviors of DOX-loaded micelles

The *in vitro* release of DOX from DOX-ss-M was investigated at 37 ℃ in 0.1 M phosphate buffer solution (PBS, pH 7.4) with or without 10 mM DTT. Typically, 1 ml DOX-ss-M solution was transferred to a dialysis tube with a MWCO of 8000-14000 and then immersed into either 25 ml PBS with no DTT or 10 mM DTT, continuously shaken (200 rpm) at 37 ℃. At desired time intervals, 3 ml of the solution was obtained from the reservoir for fluorescence measurement (excitation: 480nm, emission: 570 nm) and 3 ml of fresh media were replenished. The release experiments were conducted in triplicate, and the results presented are the average data with standard deviations. In a similar way, the release of DOX from DOX-M in PBS was also determined.

2.6 *In vitro* cytotoxicity assay

The cytotoxicity of blank micelles (NCMs and RSCMs), DOX-loaded micelles (DOX-M and cRGD-DOX-ss-M) and free DOX solution were performed by MTT assay using B16F10 cells. Cells were seeded onto 96-well plates at a density of 8000 cell per well in 100 μL of RPMI-1640 containing 10% FBS and incubated for 24 h to reach 80% confluency. The medium was removed with a fresh medium containing the empty micelles, DOX-loaded micelles and free DOX with varying concentrations. After 24 h or 48 h, the medium was replaced by 100 μL fresh RPMI-1640 and 20 μL of MTT solution (5 mg ml^{-1}) was added. After incubation for another 4 h, 150 μL of DMSO was added and shaken for 10 min. The absorbance at 570 nm of each well was measured using a microplate reader (BioTek Epoch, USA). The cell viability (%) was determined by comparing the absorbance with control wells containing only cell culture medium. Data are presented as average ± SD (n = 4). The IC_{50} value (the concentration that inhibited cell growth by 50%) of different formulation was calculated using GraphPad Prism software.

2.7 *In vitro* cellular uptake

The cellular uptake and intracellular release behaviors of the DOX-loaded micelles were investigated by confocal laser scanning microscopy (CLSM) and flow cytometry (FCM) against B16F10 cells ($\alpha_v\beta_3$ integrin-positive cells) and Hela cells ($\alpha_v\beta_3$ integrin negative cells). When examined by CLSM, B16F10 cells or Hela cells, which have been cultured in a confocal dish and incubated with different DOX-loaded micelles and free DOX. After different incubation time intervals (2h, 6h), the culture medium was removed and the cells were washed three times with PBS. Then the cells were fixed with 4% paraformaldehyde for 15 min and cell nuclei were stained with DAPI for 10 min. Confocal microscopy images were taken using CLSM (Perkin Elmer, UltraVIEW VoX ,USA).

For FCM analysis, B16F10 cells or Hela cells were seeded in 6-well plates (10^5 cells/well). After presetting incubation, the cells were collected by trypsin and centrifuged at 1000 rpm for 5 min, washed with cold PBS twice, and resuspended in 300 μL of cold PBS. Finally, the cell suspensions were filtered through 300-mesh nylon mesh and analyzed for fluorescent intensity with FCM (BD AccuriC6, USA) through the fluorescence channel 2 (FL2).

2.8 Statistical analysis

Data was expressed as means ± the standard deviation (S.D.) obtained from three separate experiments. The significances of the differences were determined using Student's t-test two-tailed for each paired experiment. A P-value < 0.05 was considered statistically significant in all cases.

3. Results and discussion

3.1 Micellization and characterization

A series of measurements were employed to verify the formations of the micelles self-assembled from amphiphilic SMA copolymers. Firstly, the NCMs, SCMs and RSCMs had a narrow size distribution in water with polydispersity index (PDI, <0.10) and an average diameter about 100 nm determined from the DLS measurement, no obvious change in size and PDI after crosslinking by cystamine or cRGD modification were observed (Table 1). Zeta potentials of the NCMs, SCMs and RSCMs determined by DLS were -26.1 mV, -33.4 mV and -31.5 mV, respectively, indicating favorable stability (Table 1). The slight decrease in zeta potential after crosslinking might be due to the existence of a small number of free carboxyl groups on the surface. Moreover, the negative surface charges of the micelles could reduce clearance by reticulo-endothelial system (RES) and prolong circulation time due to the low absorption of plasma proteins.[33] The TEM images showed that the RSCMs exhibited a spherical shape and homogeneous distribution (Fig. 2a and Fig. 2b), which was consistent with the results obtained from DLS. Using pyrene as a fluorescence probe, the CMC of the SMA micelles was determined to be 2.5 μg ml^{-1} (Fig. 2d), which guarantee the micelle to keep a favorable stability in bodily fluids before reaching tumor sites.

The stability of NCMs and SCMs against extensive dilution and organic solvent were investigated using DLS. As shown in Fig. 3a, the apparent increase in size for NCMs could be observed, wherein the size of the NCMs increased from 100 nm to 160 nm after 5000 fold dilution with water and swelled to 460 nm after 10 fold dilution with DMF. In contrast, no obvious size change was observed for SCMs upon the same volume dilution (Fig. 3b). The results suggested that SCMs could retain the micellar structure even at concentrations below the CMC or oily reagent, which is highly favored for bioapplications of micelles. In the process of intravenous administration, polymer micelles were usually susceptible to dilution below CMC, which may lead to the dissociation of micelles. [34] Therefore, the stability of the system is very important during infusion. In addition, after long-term storage at r. t. for over 6 month, there were no significant changes of SCMs in the average particle size, which demonstrated long-term stability of the SCMs.

To verify the redox-responsive cleavage of the disulfide bond in SCMs, the change of SCMs size in response to 10 mM DTT was monitored by DLS at various time

intervals. As shown in Fig. 3c, the size change was observed after 15 min, in which large aggregates with a diameter about 550 nm, and the originally unimodal peak changed into multimodal peaks in the size distribution. As time went on, the portion that represented aggregation (550 nm) increased over time. Such variation in the size was likely due to the reductive cleavage to disassemble the micelles. These results indicated that the SMA micelles crosslinked with the disulfide was able to decrosslink under a reducing environment.

The basic requirements for polymeric micelles as drug-delivery systems include high drug-loading capacity, biodegradability and controllable drug-release profiles. DOX is one of the most potent antitumor agents to treat a wide variety of solid malignant tumors by interacting with topoisomerase II, which was used as a model anti-cancer drug to evaluate the capability of the SMA micelles as a drug carrier. The SMA micelles displayed high drug loading capacity of 19.2 ± 2.1% (w/w) for hydrophobic DOX and encapsulation efficiency of 82.7 ± 1.7% (w/w). By comparison, the drug loading capacity of SMA micelles was higher than that of previously reported polymer micelles such as PEG-PCL based micelles[35] and chitosan-based polymeric micelles[36]. It might be due to that high proportion styrene of SMA could form larger hydrophilic core to load DOX through physically trapping. After crosslinking by cystamine or cRGD modification, the loading efficiency and the entrapment efficiency of DOX-ss-M and cRGD-DOX-ss-M had only slightly decreased to 14.1 ± 1.5%, 15.3 ± 2.8% and 72.1 ± 2.2%, 75.6 ± 3.1% (Table 2). However, the DOX-loaded micelles exhibited smaller size than blank micelles (76.11~80.34 nm & 95.43~106.12 nm), which may owe to hydrophobic interaction between insolubility DOX and the hydrophobic cores of polymeric micelles (Table 1 and 2). It should be noted that micelles with a small size of less than 100 nm is more likely to avoid the elimination from RES and promote the EPR effect.[37, 38]

3.2 *In vitro* drug-release behaviors of DOX-loaded micelles

The DOX release curves from the formulations (DOX-M, DOX-ss-M) were investigated in PBS (0.1 M, pH 7.4) with or without 10 mM DTT at 37 ℃. In the absence of DTT (Fig. 4), DOX-M quickly released with a 50.0% cumulative release of DOX within 8 h, followed by a slow release up to 24 h reaching about 60.0% cumulative release. The rapid release at the physiological environment (pH 7.4, PBS) due to unstability of micelles would lead to drug leakage before reaching the tumor site, therefore induce side effects and reduce therapeutic effects, which is a major challenge for micelles as drug delivery *in vivo*.[22] By comparison, the release of DOX from the DOX-ss-M was less than 25% cumulative release under the same condition over a period of 24 h. This remarkable decrease implied that the shell crosslinking of the micelles could maintain the micellar structure to entrap the drug in the hydrophobic region to prevent DOX leakage. However, in the presence of 10 mM DTT, the release rate of DOX-ss-M obviously increased, in which approximately 60% of DOX was released within 8 h. It thereby corroborated our hypothesis that DOX-ss-M could be selectively released at the tumor site under a reducing environment, which resulted from reductive cleavage of disulfide bonds.[39]

3.3 *In vitro* cytotoxicity assay

Murine melanoma B16F10 cells which overexpress integrin $\alpha_v\beta_3$[26], was used as the models of tumor neovascular endothelial cells. The biocompatibility of the blank micelles and the cytotoxicity of DOX-loaded micelles against B16F10 cells were determined by MTT assays. In Fig. 5a and 5b, both NCMs and RSCMs exhibited no obvious cytotoxicity (cell viabilities ≥ 80%) up to a tested concentration of 500 μg ml^{-1} when incubation for 24h and 48 h, indicating that the micelles as drug delivery vehicles have excellent biocompatibility and low-toxicity.

To evaluate whether the SMA micelles formulations influenced the cytotoxicity of DOX, the viability of B16F10 cells incubated with DOX-loaded micelles (DOX-M, cRGD-DOX-ss-M) and free DOX for 24 h and 48 h were determined by MTT. As shown in Fig. 5c and 5d,

both free DOX and DOX-loaded micelles caused a dose-dependent and time-dependent increase in cytotoxicity. When the concentration of DOX increased from 0.01 to 10 μg ml^{-1}, the viability of B16F10 cells incubated after 24 and 48 h with free DOX decreased from 96% to 35% and 89% to 20%, while those treated with cRGD-DOX-ss-M decreased from 95% to 11% and 82% to 4%, respectively. As expected, the viability of B16F10 cells incubated with cRGD-DOX-ss-M exhibited significantly higher toxicity than free DOX either after 24 or 48 h. The different cytotoxicity might result from the difference in their cellular uptake. Furthermore, after treatment for 48 h, the IC_{50} values of cRGD-DOX-ss-M (0.1807 μg ml^{-1}), which was 1.6 and 0.5 fold lower than the values of free DOX (0.4696 μg ml^{-1}) and DOX-M (0.2763 μg ml^{-1}) respectively. The enhanced cytotoxicity of cRGD-DOX-ss-M was attributed to cRGD peptide-mediated endocytosis and more drug release via the stimuli of reducing environment of tumor cell.

3.4 *In vitro* cellular uptake

CLSM was firstly employed to qualitatively observe the internalization process as a function of time in the αvβ3 integrin-positive cells (B16F10) and αvβ3 integrin negative cells (Hela) cultured with various DOX formulations (Fig. 6). At the same incubation time, the DOX fluorescence intensity in B16F10 and Hela cells was enhanced when DOX was loaded into micelles (Fig.6a and 6c). This difference was likely due to easier access of small particles (70-80 nm) to the cells.[38] From all the overlapped color in the merged image, the red fluorescence from various DOX-loaded micelles was visibly observed mainly in cell cytoplasm at first (Fig. 6a and 6c), but eventually the fluorescence spreading to the nuclei and distinctly increased (Fig. 6b and 6d). This may be due to that DOX-loaded micelles needed to release in the cytosol, followed by diffusion into the nuclei. Both in B16F10 and Hela cells, the redox-responsive DOX-ss-M showed higher fluorescence than DOX-M, owed to the facilitated release of DOX responding to intracellular reducing environment. Moreover, the $\alpha_v\beta_3$ integrin-positive B16F10 cells treated with cRGD-DOX-ss-M exhibit significantly higher cellular uptake than DOX-ss-M, while not in $\alpha_v\beta_3$ integrin negative Hela cells. It was a powerful proof which indicated the enhanced cellular uptake via high affinity of cRGD peptide to over-expressed $\alpha_v\beta_3$ integrin.

As expected, the quantitative flow cytometry analysis (FACS) results were also in agreement with the CLSM result. Cells without any DOX treatment only showed the auto fluorescence, so they were presented as the negative control. Both in B16F10 cells (Fig. 7) and Hela cells (Fig. 8), compared to that without redox-responsive micells, redox-responsive micells revealed higher fluorescence (DOX-ss-M & DOX-M, cRGD-DOX-ss-m & DOX-M). Furthermore, from Fig. 7a and 7b, cRGD-DOX-ss-M presented the strongest DOX fluorescence in B16F10 cells after 2 h and 6 h incubation, confirming again that the roles of integrin-mediated process in the cellular uptake and cellular redox response in the drug release. Fig. 7c and 7d demonstrated the quantitative determination of the fluorescence, we could find that the cellular fluorescence intensity in cRGD-DOX-ss-M treated cells was 1.28 and 1.53 times that of DOX-ss-M and DOX-M treated cells after 2 h, 1.60 and 2.42 times that of DOX-ss-M and DOX-M treated cells after 6 h ,respectively. While Hela Cells incubated with the cRGD-DOX-ss-M and DOX-ss-M showed equivalent fluorescence intensity after same time interval (Fig 8), which is well consistent with the CLSM assay. From all cellular uptake results, we concluded that the cRGD peptide-decorated redox-responsive polymeric micelles, cRGD-DOX-ss-M, had the ability to convey anticancer drug to target cancer cells and enhance the intracellular release.

4. Conclusions

In summary, we have demonstrated that cRGD-modified and shell-crosslinked micelles (RSCMs) based on amphiphilic polymer SMA could efficiently deliver and redox-responsed release DOX into cancer cells with $\alpha_v\beta_3$ integrin over expressing, achieving preferable antitumor effect. The terminal groups of hydrophobic chains in this copolymer were modified with c (RGDfK) peptide, resulting in a high selectivity to tumor cells that $\alpha_v\beta_3$ integrin over expressing; some hydrophobic segments were crosslinked by cystamine dihydrochloride, endowing an optimal redox-sensitivity to stimulate the intracellular drug release. A series of measurements demonstrated that the intelligent micelles possessed desirable features, including favourable stability, high drug-loading capacity, low

cytotoxicity, and controlled release property. Notably, both the cytotoxicity assay and cellular uptake analysis revealed these active targeting and redox-responsive micelles had excellent killing effect on B16F10 cells, due to the rapid deliver to the target cells and abundant release in intracellular microenvironment. Therefore, the cRGD-decorated redox-sensitive micelles have the potential to be developed as an effective targeted drug delivery system for cancer chemotherapy.

Acknowledgements

The authors would be supported by the National Natural Science Foundation of China (81201197), Hubei Province Natural Science Fund Project (2015CFB588 and 2014CFA080), and Talents Program from Hubei University of Technology (BSQD12049). The authors thank Yanghao (Ph.D.) at Huazhong University of Science and Technology, China for the helpful discussion.

Notes and references.

1 M. Ferrari, *Nature reviews. Cancer*, 2005, **5**, 161-171.
2 A. I. Minchinton and I. F. Tannock, *Nature reviews. Cancer*, 2006, **6**, 583-592.
3 S. Mura, J. Nicolas and P. Couvreur, *Nat Mater*, 2013, **12**, 991-1003.
4 H. Cabral, J. Makino, Y. Matsumoto, P. Mi, H. L. Wu, T. Nomoto, K. Toh, N. Yamada, Y. Higuchi, S. Konishi, M. R. Kano, H. Nishihara, Y. Miura, N. Nishiyama and K. Kataoka, *Acs Nano*, 2015, **9**, 4957-4967.
5 T. Wei, J. Liu, H. L. Ma, Q. Cheng, Y. Y. Huang, J. Zhao, S. D. Huo, X. D. Xue, Z. C. Liang and X. J. Liang, *Nano Lett*, 2013, **13**, 2528-2534.
6 H. Cabral and K. Kataoka, *J Control Release*, 2014, **190**, 465-476.
7 R. Plummer, R. H. Wilson, H. Calvert, A. V. Boddy, M. Griffin, J. Sludden, M. J. Tilby, M. Eatock, D. G. Pearson, C. J. Ottley, Y. Matsumura, K. Kataoka and T. Nishiya, *Brit J Cancer*, 2011, **104**, 593-598.
8 T. Hamaguchi, T. Doi, T. Eguchi-Nakajima, K. Kato, Y. Yamada, Y. Shimada, N. Fuse, A. Ohtsu, S. Matsumoto, M. Takanashi and Y. Matsumura, *Clin Cancer Res*, 2010, **16**, 5058-5066.
9 Y. H. Bae and H. Yin, *J Control Release*, 2008, **131**, 2-4.
10 S. C. Owen, D. P. Y. Chan and M. S. Shoichet, *Nano Today*, 2012, **7**, 53-65.
11 F. H. Meng, R. Cheng, C. Deng and Z. Y. Zhong, *Mater Today*, 2012, **15**, 436-442.
12 S. Bhatnagar and V. V. K. Venuganti, *J Nanosci Nanotechno*, 2015, **15**, 1925-1945.
13 L. Zhao, N. Li, K. Wang, C. Shi, L. Zhang and Y. Luan, *Biomaterials*, 2014, **35**, 1284-1301.
14 V. Torchilin, *Advanced drug delivery reviews*, 2011, **63**, 131-135.
15 E. S. Read and S. P. Armes, *Chem Commun (Camb)*, 2007, DOI: 10.1039/b701217a, 3021-3035.
16 X. Guo, C. Shi, J. Wang, S. Di and S. Zhou, *Biomaterials*, 2013, **34**, 4544-4554.
17 D. H. Kim, Y. K. Seo, T. Thambi, G. J. Moon, J. P. Son, G. Li, J. H. Park, J. H. Lee, H. H. Kim, D. S. Lee and O. Y. Bang, *Biomaterials*, 2015, **61**, 115-125.
18 Y. J. Wu, D. F. Zhou, Y. X. Qi, Z. G. Xie, X. S. Chen, X. B. Jing and Y. B. Huang, *Rsc Adv*, 2015, **5**, 31972-31983.
19 Y. G. Su, Y. W. Hu, Y. Z. Du, X. Huang, J. B. He, J. You, H. Yuan and F. Q. Hu, *Mol Pharmaceut*, 2015, **12**, 1193-1202.
20 J. Li, T. Yin, L. Wang, L. Yin, J. Zhou and M. Huo, *Int J Pharm*, 2015, **483**, 38-48.
21 Y. W. Hu, Y. Z. Du, N. Liu, X. Liu, T. T. Meng, B. L. Cheng, J. B. He, J. You, H. Yuan and F. Q. Hu, *J Control Release*, 2015, **206**, 91-100.
22 Y. P. Li, K. Xiao, W. Zhu, W. B. Deng and K. S. Lam, *Advanced drug delivery reviews*, 2014, **66**, 58-73.
23 P. Kuppusamy, H. Li, G. Ilangovan, A. J. Cardounel, J. L. Zweier, K. Yamada, M. C. Krishna and J. B. Mitchell, *Cancer research*, 2002, **62**, 307-312.
24 L. L. Wu, Y. Zou, C. Deng, R. Cheng, F. H. Meng and Z. Y. Zhong, *Biomaterials*, 2013, **34**, 5262-5272.
25 G. J. Chen, L. W. Wang, T. Cordie, C. Vokoun, K. W. Eliceiri and S. Q. Gong, *Biomaterials*, 2015, **47**, 41-50.
26 F. Danhier, A. Le Breton and V. Preat, *Mol Pharmaceut*, 2012, **9**, 2961-2973.
27 C. Y. Zhan, B. Gu, C. Xie, J. Li, Y. Liu and W. Y. Lu, *J Control Release*, 2010, **143**, 136-142.
28 N. Nasongkla, X. Shuai, H. Ai, B. D. Weinberg, J. Pink, D. A. Boothman and J. Gao, *Angew Chem Int Edit*, 2004, **43**, 6323-6327.
29 C. Rangger, A. Helbok, E. von Guggenberg, J. Sosabowski, T. Radolf, R. Prassl, F. Andreae, G. C. Thurner, R. Haubner and C. Decristoforo, *Int J Nanomed*, 2012, **7**, 5889-5900.
30 E. A. Murphy, B. K. Majeti, L. A. Barnes, M. Makale, S. M. Weis, K. Lutu-Fuga, W. Wrasidlo and D. A. Cheresh, P Natl Acad Sci USA, 2008, **105**, 9343-9348.
31 F. Danhier, B. Vroman, N. Lecouturier, N. Crokart, V. Pourcelle, H. Freichels, C. Jerome, J. Marchand-Brynaert, O. Feron and V. Preat, *J Control Release*, 2009, **140**, 166-173.
32 X. P. Duan, J. S. Xiao, Q. Yin, Z. W. Zhang, H. J. Yu, S. R. Mao and Y. P. Li, *Nanotechnology*, 2014, **25, 125-102**.
33 X. P. Duan and Y. P. Li, *Small*, 2013, **9**, 1521-1532.
34 X. X. Chuan, Q. Song, J. L. Lin, X. H. Chen, H. Zhang, W. B. Dai, B. He, X. Q. Wang and Q. Zhang, *Mol Pharmaceut*, 2014, **11**, 3656-3670.
35 N. Nasongkla, X. Shuai, H. Ai, B. D. Weinberg, J. Pink, D. A. Boothman and J. M. Gao, *Angew Chem Int Edit*, 2004, **43**, 6323-6327.
36 L. L. Cai, P. Liu, X. Li, X. Huang, Y. Q. Ye, F. Y. Chen, H. Yuan, F. Q. Hu and Y. Z. Du, *Int J Nanomed*, 2011, **6**, 3499-3508.
37 C. L. Shi, X. Guo, Q. Q. Qu, Z. M. Tang, Y. Wang and S. B. Zhou, *Biomaterials*, 2014, **35**, 8711-8722.
38 H. Cabral, Y. Matsumoto, K. Mizuno, Q. Chen, M. Murakami, M. Kimura, Y. Terada, M. R. Kano, K. Miyazono, M. Uesaka, N. Nishiyama and K. Kataoka, *Nat Nanotechnol*, 2011, **6**, 815-823.
39 R. Cheng, F. Feng, F. H. Meng, C. Deng, J. Feijen and Z. Y. Zhong, *J Control Release*, 2011, **152**, 2-12.

Graphical abstract

Table 1 Size and zeta potential of blank micelles determined by DLS.

Table 2 Characteristics of DOX-loaded micelles.

Fig. 1 Schematic illustration of cRGD-functionalized redox-sensitive core-crosslinked SMA micelles for active loading and intracellular microenvironment triggered release of DOX.

Fig. 2 (a), (b) TEM image of RSCMs at different magnification. (c) Size distribution of RSCMs by DLS. (d) CMC of RSCMs derived from the plot of I_{384}/I_{373} rat io vs micelle concentration using pyrene as a probe.

Fig. 3 Comparison of stability of of NCMs (a) and SCMs (b) against dilution by water (5000 fold) and DMF (10 fold). (c) Redox-induced size variation of SCMs in response to 10 mM DTT with time followed by DLS.

Fig. 4 In vitro release of DOX in the presence or absence of 10 mM DTT from DOX-ss-M and DOX-M. Data are presented as mean ± SD (n=3).

Fig. 5 Cytotoxicity of blank micelles (NCMs and RSCMs), DOX-loaded micelles (DOX-M and cRGD-DOX-ss-M) and free DOX using B16F10 cells. (a) blank micelles, 24 h incubation, (b) blank micelles ,48 h incubation, (c) drug loaded micelles and free DOX, 24 h incubation, (d) drug loaded micelles and free DOX, 48 h incubation. Data are presented as mean ± SD (n=3).

Fig. 6 Confocal laser scanning microscope images of B16F10 cells ($\alpha_v\beta_3$ intergrin-positive)((a) 2h, (b) 6 h) and Hela cells ($\alpha_v\beta_3$ intergrin-negative)((c) 2h, (d) 6 h) that were treated with free DOX and DOX-loaded micells. Nuclei were stained with DAPI. DAPI staining images and DOX images were merged.

Fig. 7 Flow cytometry analyses and mean fluorescence intensity contrasting the level of cellular uptake between B16F10 cells incubated with free DOX and various DOX loaded micelles for 2 h ((a) and (c)) and 6 h ((b) and (d)).Statistical significance:*$P<0.05$，**$P<0.01$.

Fig. 8 Flow cytometry analyses and mean fluorescence intensity contrasting the level of cellular uptake between Hela cells incubated with free DOX and various DOX loaded micelles for 2 h ((a) and (c)) and 6 h ((b) and (d)).Statistical significance:*$P<0.05$，**$P<0.01$.

Table 1

Sample	Size (nm)	PDI	Zeta potential(mV)
NCMs	104.50 ± 2.13	0.093 ± 0.025	-26.1 ± 1.8
SCMs	95.43 ± 4.58	0.073 ± 0.041	-33.4 ± 1.9
RSCMs	106.12 ± 3.75	0.087 ± 0.041	-31.5 ± 3.2

Table 2

Sample	Size (nm)	PDI	Zeta potential (mV)	DLC (%)	DLE (%)
DOX-M	80.34 ± 4.32	0.169 ± 0.032	-29.1 ± 2.3	19.2±2.1	82.7±1.7
DOX-ss-M	69.64 ± 5.56	0.178 ± 0.029	-37.6 ± 3.5	14.1±1.5	72.1±2.2
cRGD-DOX-ss-M	76.11 ± 3.77	0.176 ± 0.052	-35.5 ± 2.2	15.3±2.8	75.6±3.1

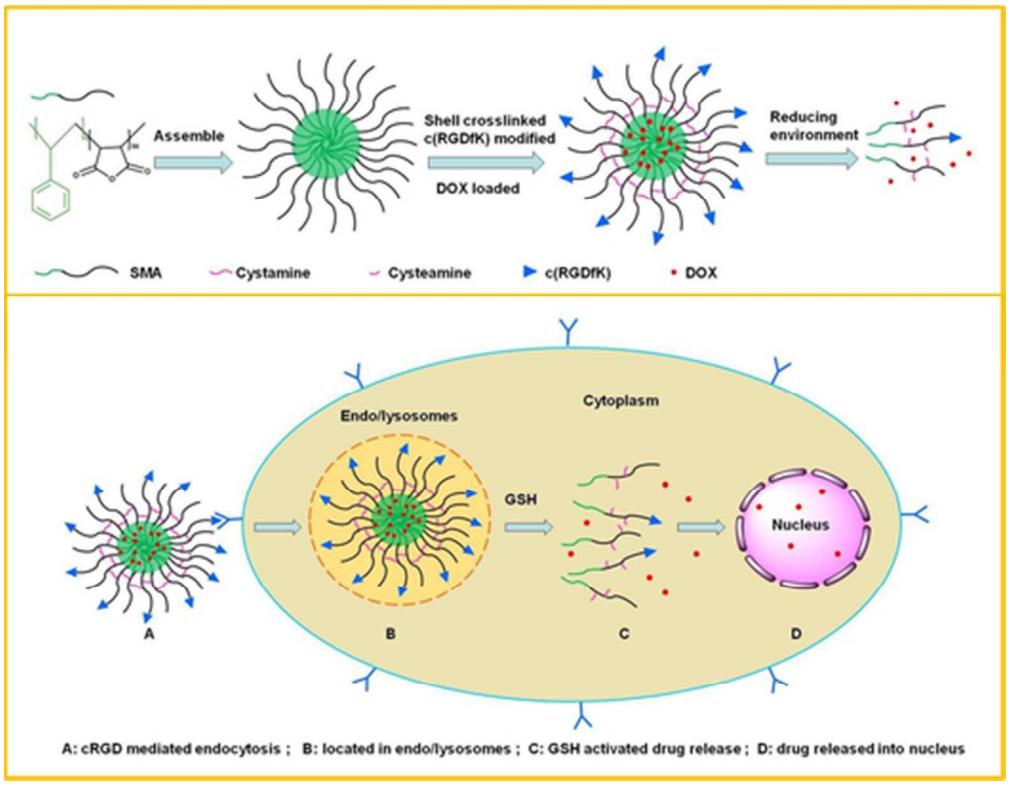

44x34mm (300 x 300 DPI)

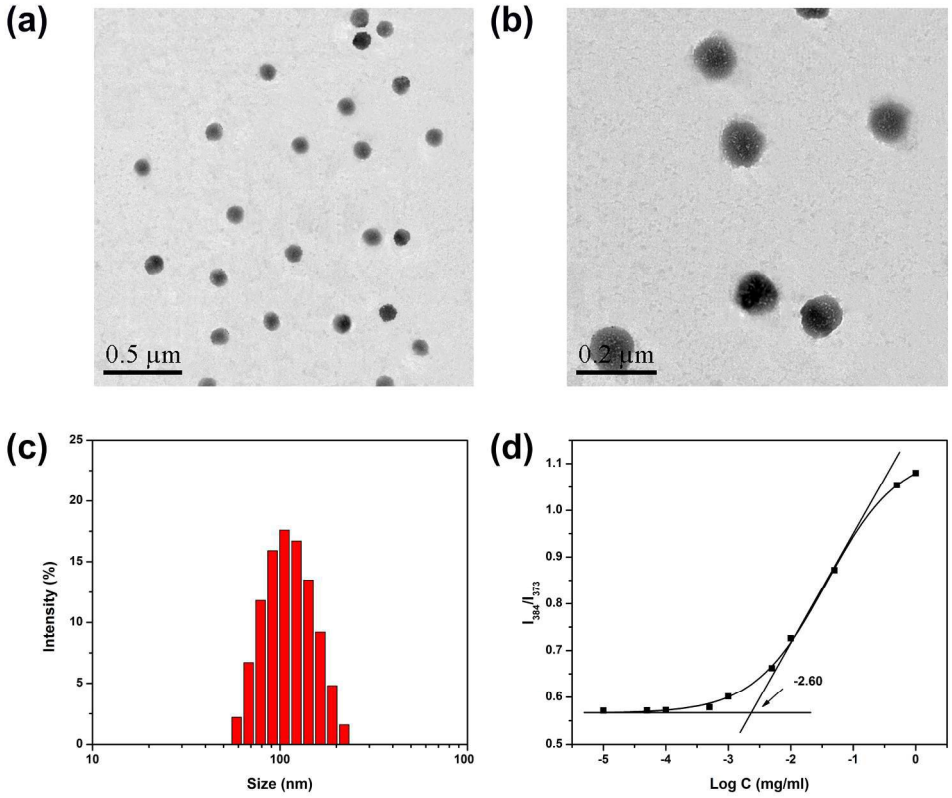

212x176mm (300 x 300 DPI)

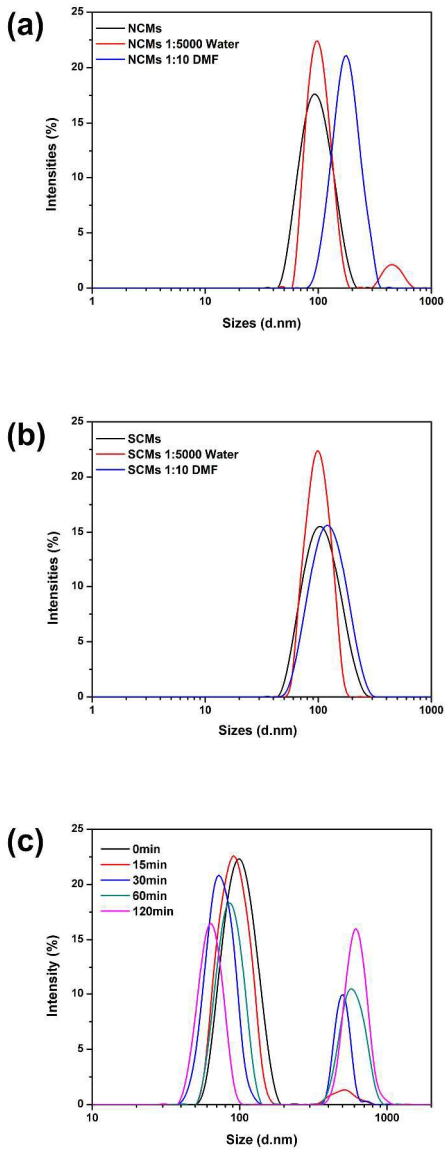

337x816mm (300 x 300 DPI)

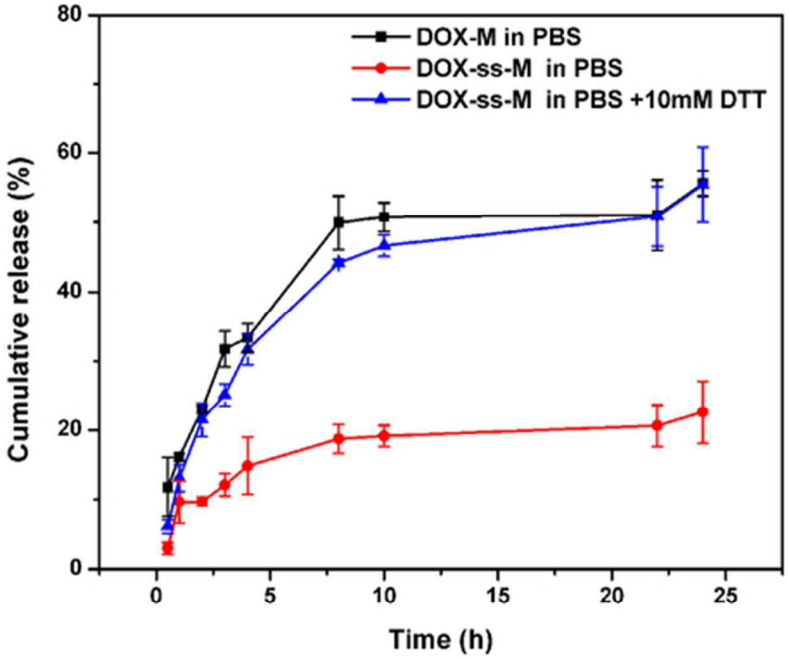

49x37mm (300 x 300 DPI)

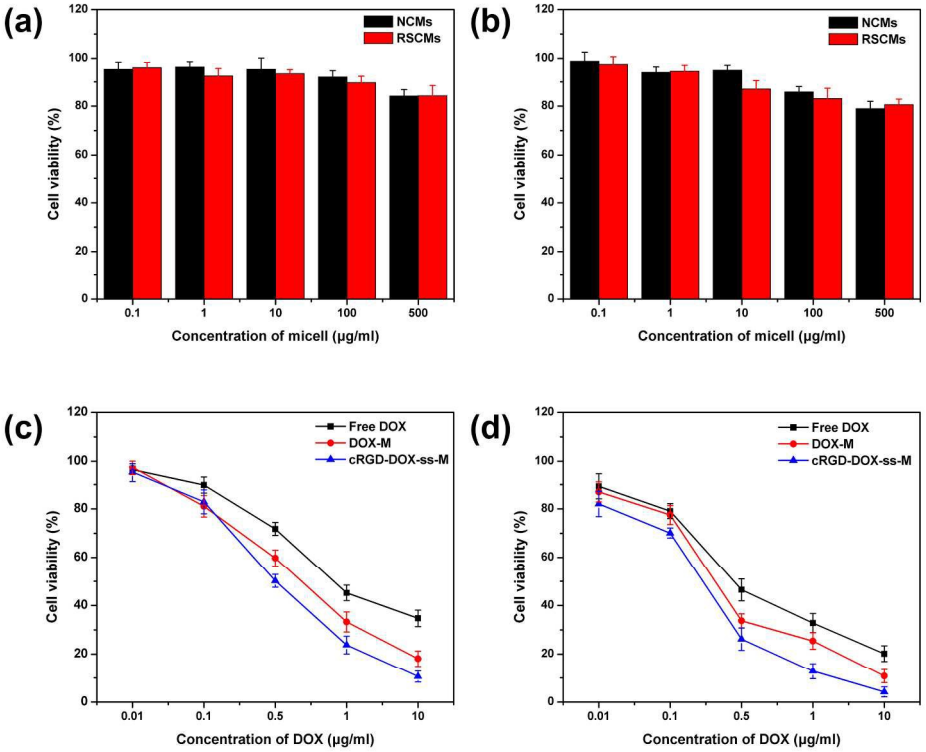

215x174mm (300 x 300 DPI)

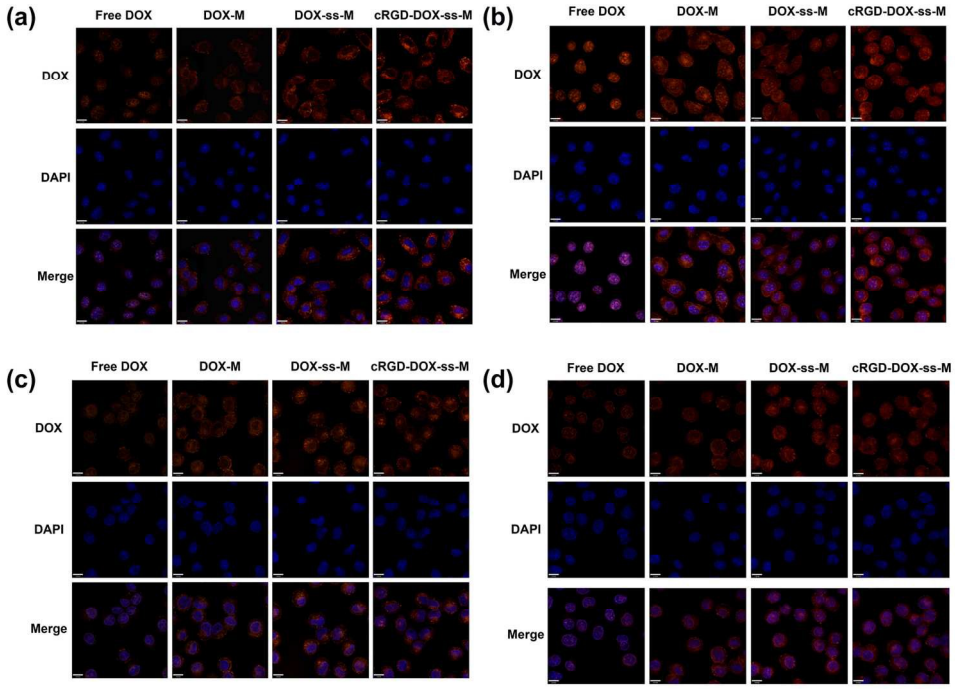

151x111mm (300 x 300 DPI)

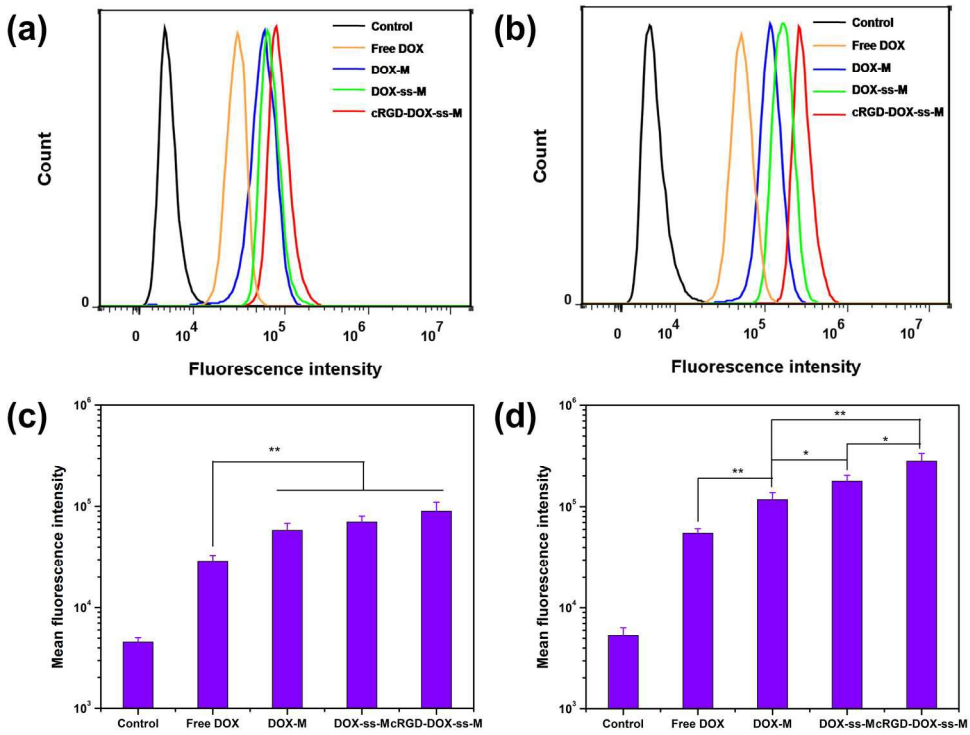

201x158mm (300 x 300 DPI)

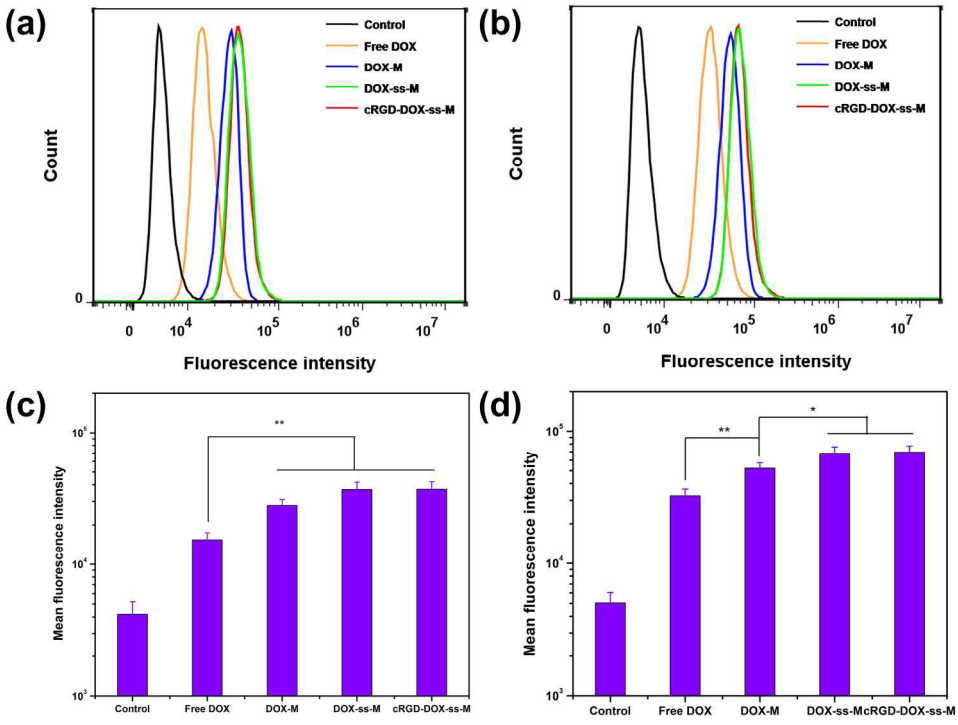

197x152mm (300 x 300 DPI)